

Evgeniy Mokrov, Irina Gudkova

Peoples Friendship University of Russia, Moscow, Russia

PERFORMANCE EVALUATION OF DYNAMIC LSA OPERATION THROUGH A MODEL OF A STAND-ALONE CELL*

ABSTRACT

This paper considers an analytical model of an LTE network using LSA concept to gain access to the airport spectrum according to the limit power algorithm with signal-interference ratio threshold as a stand-alone cell during the airplane takeoff. User transmission power and transmission rate plots against time are presented for different cell locations for two different signal propagation models.

KEYWORDS

LTE; path loss; LSA; interference; limit power.

Мокров Е.В., Гудкова И.А.

Российский университет дружбы народов, г. Москва, Россия

ОЦЕНКА ПРОИЗВОДИТЕЛЬНОСТИ РАБОТЫ LSA НА ПРИМЕРЕ МОДЕЛИ ОТДЕЛЬНО ВЗЯТОЙ СОТЫ

АННОТАЦИЯ

В данной статье построена аналитическая модель сети LTE, использующей мощности аэропорта по технологии LSA, согласно алгоритму ограничения мощности, с пороговым значением на отношение сигнала к интерференции на примере отдельно взятой соты в моменты взлета самолета. Приведены графики изменения мощностей и скоростей абонентов для различных положений рассматриваемой соты в зависимости от времени.

КЛЮЧЕВЫЕ СЛОВА

LTE; затухание сигнала; LSA; интерференция; снижение мощности.

In this paper, we study an LSA use case, where the airport owns a spectrum license over a large area and uses it for the telemetry when airplanes take-off. There is a cellular network present in the area where the airplane receives telemetry signals, and the respective mobile network operator (MNO) has means to constrain its interference towards the airplanes. Also we assume that planes take-off only occasionally, that is, only one airplane is present in the MNO coverage at once. Thus the spectrum is used in small and localized area around the airplane. In the considered scenario, a mobile network uses an airports telemetry spectrum until an airplane needs to receive telemetry signal from the air traffic control. When it happens, the MNO restricts interference its user equipment (UE) causes around the position of the airplane, to let it receive the telemetry signal. To this end, MNO uses limit power policy [1]. The MNO reduces its UE power for users using LSA band in this area. Also note that here we consider two signal propagation models – two-ray ground-reflection model and free-space path loss model. The results on power and transmission rate were derived and compared for both models.

Table 1 represents the notations used further in the paper. Note that while function $p_u^{lx}(t)$ is the reduced power of the UE, constant p_u^{lx} is the initial UE power.

Table 1. Notations

Notations	Value	Description
Airport parameters		

* Proceedings of the I International scientific conference "Convergent cognitive information technologies" (Convergent'2016), Moscow, Russia, November 25-26, 2016

f	2.1 GHz	carrier frequency
G_a	3	airport antenna gain
h_a	20 m	height on which the airport transmitter is located
p_a^{tx}	24.39 dBm [2]	power of the airport transmitter
v_0	65 m/s	airplane take-off speed
a	5 m/s	airplane acceleration
β	7 deg [1]	airplane ascent angle
SIR_0	15 dB	signal-interference ratio (SIR) threshold for the airplane
	Two-ray ground-reflection model Free-space path loss	signal propagation model
γ	15 deg	take-off runway turn angle towards x axis
$(x_a, y_a, 0)$	(0,0,0)	position of the airport
$(x(t), y(t), z(t))$		position of the airplane at time t
$d_a(t)$		distance between the airplane and the airport at time t
$p_a^{rx}(t)$		power received by the airplane from the airport at time t
Operator parameters		
r_c	288 m [1]	cell radius
G_c	18	BS transmitter Gain
h_c	10 m	height on which the BS transmitter is located
h_u	1.5 m	height on which the UE is located
p_u^{tx}	23 dBm	power of the user equipment
$(x_c, y_c, 0)$		position of eNodeB
$p_u^{tx}(t)$		power received by airplane from the cell user at time
$d_c(t)$		distance between the airplane and eNodeB at time
$D_c(t)$		projection of the distance between the airplane and eNodeB at time t towards vector i
$d(t)$		distance between the airplane and the closest user at time t
$SIR(t)$		SIR for the airplane at time t
$d_u(t)$		distance between the airplane and the closest edge user at time t
$D_u(t)$		projection of the distance between the airplane and the closest edge user at time t towards vector i
$\overline{p_u^{tx}}(t)$		reduced power of the user equipment at time t
C	20 MGz	channel bandwidth
w	16.8 Mb/s	initial downlink transmission rate
$w(t)$		downlink transmission rate at time t

The airport is located at the coordinates (x_a, y_a) and it has a transmitter that sends telemetry signals to the airplanes during take-off. The transmitter power is p_a^{tx} , the carrier frequency is f . Airplane

takes off with speed v_0 , acceleration a and ascending angle β following trajectory j (Fig. 1). The runway is facing along the vector i . There is a mobile operator network in the area around the airport. This operator uses LSA and transmits on the same frequency as the airport. The eNodeB has a directional transmitter that does not interfere with the signals the airplane receives from the airport. The UE have omnidirectional transmitter that transmits with power p_u^{tx} and can interfere with the airplanes in the vicinity. Let us consider the worst-case scenario for a stand-alone cell when the user interfering with the airplane holds closest to the airplane position in the cell. Target cell eNodeB is located at the coordinates (x_c, y_c) , the cell have radius r_c .

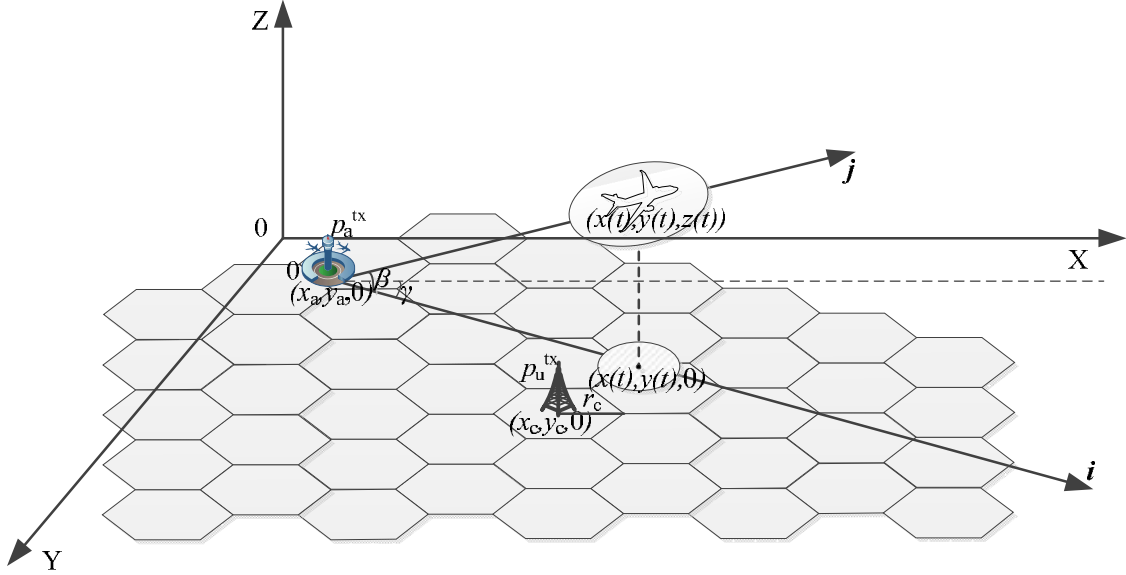


Fig. 1. LSA use-case scenario

The UE interferes with the telemetry signal and the interference threshold is given by its respective SIR value SIR_0 . That means that if the SIR on the airplane $SIR(t)$ at time t reaches the threshold SIR_0 the transmitting power of the users' equipment will be reduced so that the SIR value for the plane is goes up to the threshold. When the SIR on the plane exceeds the threshold value SIR_0 , the power of the UE can be restored. Thus we need to determine the timeslot when the cell interference towards airplane causes SIR reduction below the threshold SIR_0 .

Let the airplane at time t be located at the coordinates $(x(t), y(t), z(t))$. Knowing the airplane starting position and all its starting data we can obtain its position as

$$x(t) = x_a + \left(v_0 t + \frac{at^2}{2} \cos\beta \right) \cos\gamma, \quad (1)$$

$$y(t) = y_a + \left(v_0 t + \frac{at^2}{2} \cos\beta \right) \sin\gamma, \quad (2)$$

$$z(t) = \frac{at^2}{2} \sin\beta. \quad (3)$$

Let us denote the distance between the airplane and the eNodeB as

$$d_c(t) = \sqrt{(x(t) - x_c)^2 + (y(t) - y_c)^2 + (z(t) - h_c)^2}, \quad (4)$$

distance between the airplane and the closest edge user,

$$d_u(t) = \sqrt{\left(\sqrt{d_c^2(t) - z^2(t)} - r_c \right)^2 + (z(t) - h_u)^2}, \quad (5)$$

and the distance between the airplane and the airport

$$d_a(t) = \sqrt{(x(t) - x_a)^2 + (y(t) - y_a)^2 + (z(t) - h_a)^2}. \quad (6)$$

These distances can be seen in Fig. 2, which presents a side view projection along the airplane's trajectory.

Considering two-ray ground-reflection model (PL), path loss of the signal that travels distance d can be found using the following formula

$$PL(d) = 10 \lg \left(\frac{d^4}{G z^2(t) h^2} \right), \quad (7a)$$

for free-space path loss model (FSPL) path loss is derived from formula

$$FSPL(d) = 20 \lg \left(\frac{4\pi f d}{c} \right), \quad (7b)$$

where $c = 3 \cdot 10^8$ – speed of light.

Considering the above introduced notations algorithm to estimate the UE power reduction level can be presented as follows.

Using formulas (7a), (7b) we can obtain the signal received by the airplane from the airport at time t . For PL model it can be written as

$$p_a^{rx}(t) = p_a^{tx} - PL(d_a(t)), \quad (8a)$$

and for FSPL model it is

$$p_a^{rx}(t) = p_a^{tx} - FSPL(d_a(t)). \quad (8b)$$

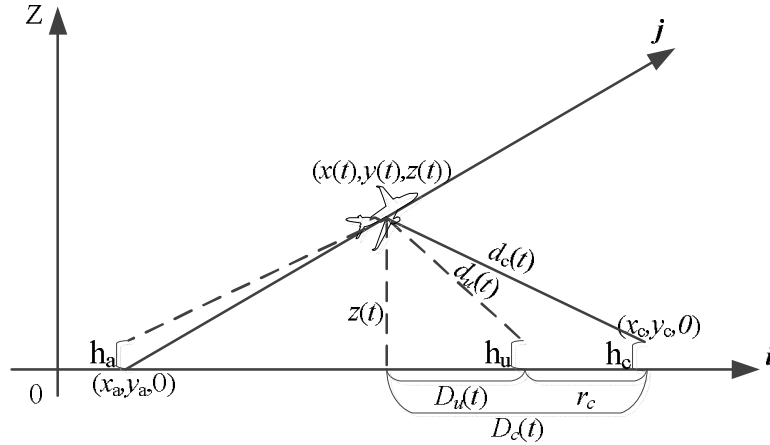


Fig. 2. Model notations for the stand-alone cell scenario

Using formulas (8) and (7) we can acquire distance $d(t)$ as

$$d_u(t) = PL^{-1} \left(p_u^{tx} - p_u^{rx}(t) \right) = 10 \left(\frac{p_u^{tx} - p_u^{rx}(t)}{40} \right) \sqrt[4]{G_a z^2(t) h_u^2} \quad (9a)$$

for PL, and

$$d_u(t) = FSPL^{-1} \left(p_u^{tx} - p_u^{rx}(t) \right) = \frac{c}{4\pi f} 10^{\frac{p_u^{tx} - p_u^{rx}(t)}{20}} \quad (9b)$$

for FSPL. Note that in case of FSPL model we disregard the height of the antennas since it have close to no effect the end result.

Since we consider case when SIR $SIR_0 = p_a^{rx}(t) - p_u^{rx}(t)$ we can express $p_u^{rx}(t)$ as

$$p_u^{rx}(t) = p_a^{rx}(t) - SIR_0 \quad (10)$$

Let's also denote the projection of the distance from the airplane to the eNodeB towards vector i (Fig. 2):

$$D_c(t) = \sqrt{d_c^2(t) - z^2(t)} \quad (11)$$

Now we can find the distance between the airplane and the closest user in cell. There are two possible cases.

Case A. if $D_c(t) \leq r_c$, that is the airplane is located directly above the cell. In this case since we consider the worst-case scenario, the closest user is located directly below the airplane. In this case the

distance between the airplane and the closest user equals the flight height, that is $d_u(t) = z(t)$ (Fig. 3A).

Case B. If $r_c < D_c(t)$, that is the airplane is located close enough to the cell to experience high interference, but it is not located directly above the cell (Fig. 3B). In this case the distance between the airplane and the closest user equals the distance between the airplane and the cell edge $d(t) = d_u(t)$.

$$\text{Thus } d(t) = \begin{cases} z(t), D_c(t) \leq r_c, \\ d_u(t), D_c(t) > r_c. \end{cases} \quad (12)$$

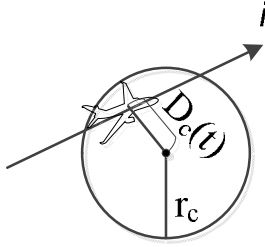


Fig. 3A. Above the cell

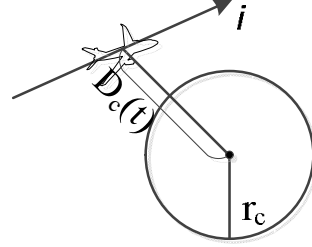


Fig. 3B. Outside the cell

Fig. 3 Cell-relative airplane position

Knowing the distance to the closest user, using formulas (8a), (8b) we can calculate SIR for each moment of time:

$$SIR(t) = p_a^{rx}(t) - p_u^{rx}(t), \quad (13)$$

Thus using expression (12) with SIR threshold SIR_0 and setting $\overline{p_u^{rx}(t)} = \overline{p_u^{rx}(t)}$ we can obtain a formula to calculate the UE power reduction level $\overline{p_u^{rx}(t)}$ as follows:

$$\overline{p_u^{rx}(t)} = \min\{p_a^{rx}(t) - SIR_0 + PL^*(d_u(t)), p_u^{tx}\}, \quad (14)$$

After that we can use Shannon formula to calculate maximal downlink (DL) transmission rate in the cell as

$$w(t) = C \ln \left(1 + 10 \frac{p_u^{tx}(t) - PL^*(r_c) - I}{10} \right), \quad (15)$$

where interference towards user signal I can be considered constant and obtained by using initial DL transmission rate as

$$I = p_u^{tx} - PL^*(r_c) - 10 \lg \left(e^{\frac{w}{C}} - 1 \right). \quad (16)$$

Note, that in formulas (14), (15), (16) PL^* is the formula for path loss substituted with (7a) or (7b) depending on the model considered.

Further we present a numerical analysis for several different locations of eNodeB. The input data is presented in Table 1 and the eNodeB locations can be seen on figure Fig. 4. Fig. 5 shows the case when the cells are located directly along the airplane's path and have the highest Interference towards the plane. For most of these cells at some time interval the airplane is located directly above them (Case A). Fig. 5A shows UE transmission power variation and worst case transmission power for cells along the airplanes trajectory marked on Fig. 4 for free space path loss model, Fig. 5B shows DL transmission rate variation and worst case transmission rate for the same cells under FSPL model. Fig. 5C and Fig. 5D show worst case UE transmission power and DL transmission rate for the marked cells under two-ray ground-reflection model. The dashed lines shows transmission power and DL transmission rate variation for each marked cell, while the solid line outlines the minimal possible values across all cells. The last cell can correspond to the coverage boundary.

It can be seen that while considering FSPL model the power rapidly drops at the takeoff and only starts rising when the airplane leaves the corresponding cell, and even after that the power never comes up to the initial value, until the airplane fully leaves the area. Although in this case we never actually shut down a cell, as it can be seen on Fig. 5B the actual transmission rate is very low until the airplane vacates the spectrum.

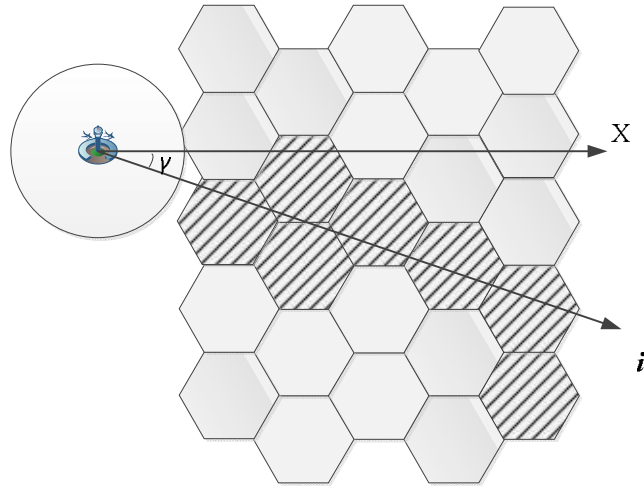


Fig.4 Cell locations respective to the airplane trajectory

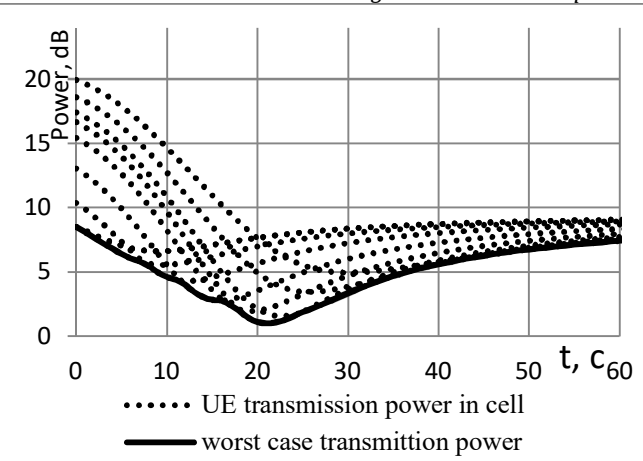


Fig. 5A Transmission power along the airplane trajectory under free space path loss model

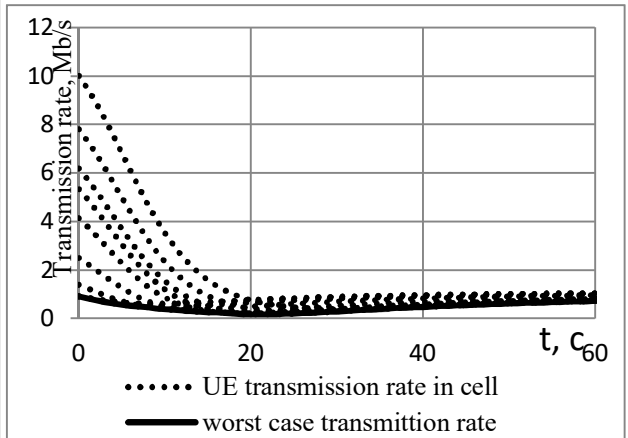


Fig. 5B Transmission rate along the airplane trajectory under free space path loss model

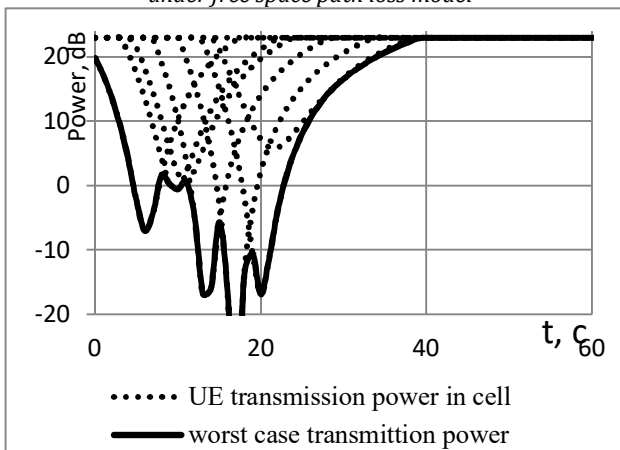


Fig. 5C Transmission power along the airplane trajectory under two-ray ground-reflection model

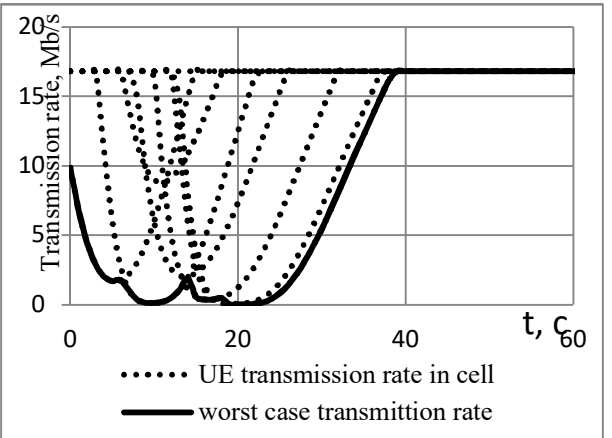


Fig. 5D Transmission rate along the airplane trajectory under two-ray ground-reflection model

Fig. 5 Transmission power and transmission rate variations in cells along the airplane's trajectory

In case of two-ray ground-reflection model both power and transmission rate rapidly decreases when the airplane approaches the cell and it steadily grows as the airplane leaves the cell. Although for this model the decrease and grow of both transmission power and transmission rate are much faster, it is evident from the plots, that nonetheless maximal value is still never reached, since it would make the interference towards the airplane too strong. Basically, both models follow the same path, although values given by the two-ray ground-reflection model are higher, which in turn tells us that the estimation derived from this model might be better suited for our scenario. This conclusion is partially proved by an LSA simulation

experiment conducted on the fully-functional 3GPP LTE cellular deployment in Brno University of Technology is described in [3], since for the 2 cell network the transmission rate of one cell was relatively high, even when the second cell was shut down. The graphs for DL transmission rate resembles those obtained in [3] with the exception of asymmetry of the presented graph, which can be explained by using SIR instead of received interference as the licensee QoS parameter. Also comparing two graphs an offset can be observed. This offset is caused by the fact that in [3] data recording ended upon reaching the furthest part of the second cell, while in present paper we consider longer time interval.

In this paper we studied a stand-alone cell scenario for limit power policy with SIR as the licensee QoS parameter for LTE network using LSA. Numerical analysis shows that for the cells along the airplane's path transmission power and DL transmission rate would be minimal for those, whose centers are directly located under the airplane, while for the cells located away from the airplane's trajectory the worst case would be reached for the cell, closest to the airplane trajectory. Also it was shown, that the two-ray ground-reflection model gives us better estimation of the power behavior for the considered scenario, and periods of sharp power and transmission rate reduction for this model are comparatively short, so it is still possible to use the spectrum even when it is simultaneously used for telemetry if SIR is used as the licensee QoS parameter by the airport, although the transmission rate would be lower compared to the case of vacant spectrum.

References

1. Aleksei Ponomarenko-Timofeev, Alexander Pyattaev, Sergey Andreevy, Yevgeni Koucheryavy, Markus Mueck, Ingolf Karls. Highly Dynamic Spectrum Management within Licensed Shared Access Regulatory Framework. IEEE Communications Magazine 54(3), p.100-109, 2016.
2. International Civil Aviation Organization Working Paper of Aeronautical Communications Panel (ACP). Third Meeting of the Surface Datalink Working Group on Considerations on Power Output versus Interference Potential, Montreal, Canada 09-11 July 2013
3. Pavel Masek and Evgeny Mokrov and Alexander Pyattaev and Krystof Zeman and Aleksei Ponomarenko-Timofeev and Andrey Samuylov and Eduard Sopin and Jiri Hosek and Irina A. Gudkova and Sergey Andreev and Vit Novotny and Yevgeni Koucheryavy and Konstantin Samouylov. Experimental Evaluation of Dynamic Licensed Shared Access Operation in Live 3GPP LTE System, IEEE GLOBECOM, accepted paper.

Литература

1. Алексей Понаморенко-Тимофеев, Александр Пятаев, Сергей Андреев, Евгений Кучерявый, Маркус Муэк, Ингольф Карлс. Highly Dynamic Spectrum Management within Licensed Shared Access Regulatory Framework. IEEE Communications Magazine 54(3), p.100-109, 2016.
2. International Civil Aviation Organization Working Paper of Aeronautical Communications Panel (ACP). Third Meeting of the Surface Datalink Working Group on Considerations on Power Output versus Interference Potential, Montreal, Canada 09-11 July 2013.
3. Павел Машек, Евгений Мокров, Александр Пятаев, Кристоф Земан, Алексей Понаморенко-Тимофеев, Андрей Самуйлов, Эдуард Сопин, Иржи Госек, Ирина А. Гудкова, Сергей Андреев, Вит Новотный, Евгений Кучерявый, Константин Самуйлов. Experimental Evaluation of Dynamic Licensed Shared Access Operation in Live 3GPP LTE System, IEEE GLOBECOM, accepted paper.

Поступила 21.10.2016

Об авторах:

Мокров Евгений Владимирович, ассистент кафедры прикладной информатики и теории вероятностей факультета физико-математических и естественных наук Российского университета Дружбы Народов, melkor77@yandex.ru;

Гудкова Ирина Андреевна, доцент, доцент (международного уровня) кафедры прикладной информатики и теории вероятностей факультета физико-математических и естественных наук Российского университета Дружбы Народов, кандидат физико-математических наук, igudkova@sci.pfu.edu.ru.